Efficiency Map based Modelling of Electric Drive for Heavy Duty Electric Vehicles and Sensitivity Analysis

Abhay, Nived ; Dong, Jianning; Bauer, Pavol; Nouws, Simon

DOI
10.1109/ITEC51675.2021.9490191

Publication date
2021

Document Version
Final published version

Published in
2021 IEEE Transportation Electrification Conference & Expo (ITEC)

Efficiency Map based Modelling of Electric Drive for Heavy Duty Electric Vehicles and Sensitivity Analysis

Nived Abhay*, Jianning Dong *, Pavol Bauer * and Simon Nouws†
* Faculty of Electrical Engineering, Mathematics and Computer Science,
Delft University of Technology, 2628 CD Delft, The Netherlands
Email: nived.abhay@gmail.com, j.dong-4@tudelft.nl, p.bauer@tudelft.nl

† DAF Trucks NV, 5643 TW Eindhoven, Netherlands
Email: simon.nouws@daftrucks.com

2021 IEEE Transportation Electrification Conference & Expo (ITEC) | 978-1-7281-7583-6/21/$31.00 ©2021 IEEE | DOI: 10.1109/ITEC51675.2021.9490191

***Abstract*—This paper presents a method to model losses of the electric drive for electric vehicles from the limited information provided in the efficiency map. A Particle Swarm Optimisation (PSO) algorithm and simple loss model based method is used to extract the loss coefficients from the motor drive efficiency map. The copper loss, hysteresis loss, eddy current loss and windage loss of the motor and switching and conduction losses of the inverter are considered. The method is used to analyze how to increase the range of heavy duty electric trucks. Sensitivity analysis is performed to identify the key parameters contributing to the range. Influence of different powertrain architectures on the range are studied. The proposed method proves to be effective. Comapred to directly applying the efficiency map, the proposed method provides more insigts into the loss distribution in the inverters and motors, reveals the key factors influencing the powertrain loss and can be used to guide the optimisation of the powertrain architecture and motors for future designs.**

I. Introduction

Heavy-duty vehicles play an important role in global and urban emissions in the transportation sector. Nowadays, more tractor manufacturers are joining the electrification transition and building their medium-duty and heavy-duty battery electric vehicles (BEV). Software modelling and testing of electric drive module prototypes enable risk reduction and demonstrate whether or not specific designs are viable in an early stage, thus accurate modelling of the loss in each powertrain component is necessary [1].

The efficiency map of the powertrain components is often used in industry to estimate the energy efficiency or range of the vehicle. However, how the detailed loss distribution in the inverter and the motor is unknown if the efficiency map is used as a black-box. A comprehensive knowledge on these losses and their share are necessary for the design and optimisation process to improve range. The information can be obtained from experiments or finite element modelling methods [2]. However, with limited information accessed from subsystem manufacturers, such as the efficiency map and the motor rating, this approach is not feasible.

This paper presents a method to extract the loss models of electrical powertrain components from the efficiency map. By combining loss models with the efficiency map, loss coefficients are identified using the Particle Swarm Optimisation (PSO) algorithm. Compared to the black-box like efficiency map, the loss models with extracted coefficients provide an insight into the key influence factors of the losses and their share in the powertrain components. Then the loss models are used to estimate the range of the truck.

Based on the extracted models, the paper investigate into the range extension of the heavy-duty BEV by comparing different vehicle parameters and powertrain architectures. A simulation based sensitivity analysis is performed by varying the vehicle parameters to understand its influence on energy efficiency and driving range of the BEV. The simulation results are observed for a specific driving profile provided by the manufacturer and validated by the real-world driving range data. Finally, a comparison with two other possible powertrain architectures is presented and their results are discussed. Compared to existing methods for range estimation and sensitivity study based on detailed models or only efficiency maps, the proposed method is able to link the loss with the underline physics and provide a possibility to guide the powertrain optimisation when limited information is available.

In Section II, the models for individual losses will be presented, and how PSO is used to extract the loss coefficients from the efficiency map is shown. A sensitivity study based on the developed models will be carried out in Section III. In Section IV, two powertrain architectures will be compared based on the analysis. Then the conclusion is drawn in Section V.

II. Loss Modelling and Parameter Identification

The investigated powertain uses an voltage source inverter driven permanent magnet synchronous machine (PMSM). A 200 kW motor from Siemens ELFA series is chosen and IGBT modules compatible to its power rating is chosen from Semikron International for the inverter. Main specifications of the PMSM drive and its reference efficiency map are shown in Table I and Figure 1 respectively.

TABLE I
MAIN SPECIFICATIONS OF INVESTIGATED PMSM DRIVE

Parameters	Values
Rated voltage	650 V
Rated current	300 A
Rated power	200 kW
Max. power	240 kW
Rated torque	2000 Nm
Max. torque	3800 Nm
Max. speed	3500 r/min

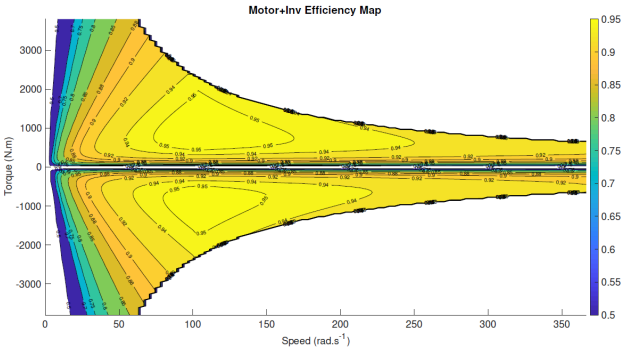

Fig. 1. Efficiency map of the investigated motor drive.

A. Motor loss calculation

1) Copper Loss: copper loss is due to the electrical resistance in the winding, which is proportional to the square of the current flowing through the three phases. At low speed the current can be considered to be proportional to the current, so

$$\text{Copper loss} = 3I^2R_s = k_cT^2, \tag{1}$$

where k_c is a constant of proportionality which is dependent on the resistance of the winding and the magnetic flux, T is the torque. In the flux weakening region the right most part of (1) is invalid. Therefore, the stator resistance R_s is calculated by dividing the copper loss with current at low speeds. The current calculation is explained in Subsection II-C. Using the calculated stator resistance and the changing current value, the copper loss in the flux-weakening region is calculated.

2) Iron Loss: Iron Loss: The iron loss model is derived based on the iron loss equation by neglecting the excess loss [3], [4]:

$$\text{Eddy current loss} = k_{ed}\omega^2, \quad \text{Hysteresis loss} = k_h\omega, \tag{2}$$

where k_{ed} and k_h are proportionality constants, and ω is the motor angular speed.

3) Friction and Windage Loss: The power loss from these two resistive torques is calculated by multiplying with the angular velocity and hence the following is obtained:

$$\text{Friction loss} = T_f\omega, \quad \text{Windage loss} = k_w\omega^3 \tag{3}$$

Here, T_f is the friction torque and k_w is constant which is obtained from the size and shape of the motor and is also dependant on the presence of a cooling fan.

Since both the hysteresis loss and the friction loss are proportional to the angular speed, they can be combined into one term for modelling. Hence, the overall equation can be written as

$$\text{Motor loss} = k_cT^2 + k_h\omega + k_{ed}\omega^2 + k_w\omega^3 \tag{4}$$

Be aware that the copper loss in the field weakening region has to be tackled separately.

B. Inverter Loss Model

This paper elaborates on the switching and conduction loss calculation of individual IGBT and reverse recovery diode which is further scaled to estimate the total inverter loss of a two-level three-phase inverter. The modulation technique for the inverter considered is sinusoidal pulse width modulation.

Losses in the driver circuit and passive components including the filter inductor or capacitor are assumed to be negligible. On-state conduction loss, turn-on and turn-off switching losses are considered for IGBTs and the on-state conduction loss and turn-off (reverse recovery) losses are considered for diodes. The reverse blocking losses of the IGBTs and the turn-on losses of the diodes are assumed to be negligible. The diodes are assumed to have a fast diode turn-on process and hence the turn-on losses are neglected in the following method.

- IGBT and diode switching times and dead-time are neglected;
- Junction temperatures are assumed to constant throughout the operation;
- Switching ripples of the currents are neglected.

1) Conduction Losses: The conduction losses are contributed by the IGBT and the diode in the IGBT module together:

$$P_{\text{cond, total}} = P_{\text{cond, diode}} + P_{\text{cond, IGBT}}. \tag{5}$$

The conduction loss can be calculated from the current flowing through the device i_{ds}, their on-state resistance R_{on} and forward voltage V_f:

$$P_{cond} = V_d i_d + R_{on} i_{ds}^2 \tag{6}$$

Duty cycles of the devices have to be considered in the calculation, which is able to be derived from the modulation index, as shown in [5].

2) Switching Losses: The turn-on and turn off loss per switching period per device can be calculated as [6], [7].

$$P_{sw} = f_{sw} \times E_{on+off} \frac{\sqrt{2}}{\pi} \times \left(\frac{I_m}{\sqrt{2}I_{ref}}\right)^{K_i} \times \left(\frac{V_{DC}}{V_{ref}}\right)^{K_v} \times \left(1 + TC_{sw}.(T_j - T_{ref})\right), \tag{7}$$

where E_{on+off} represents energy lost during turn-on and turn-off of IGBT or the reverse recovery E_{rr} energy of the diode, f_{sw} is the switching frequency, K_i and K_v are the current and voltage dependencies of switching loss respectively, I_m is the amplitude of the inverter current, V_{DC} is the DC voltage and V_{ref} and I_{ref} are the reference DC voltage and DC current respectively to which the energy lost correlates.

TC_{sw} is the temperature coefficient for switching losses, T_j is the junction temperature and T_{ref} is the reference value of temperature. Those parameters are set based on the reference values available in the datasheet of the IGBT module.

The IGBT turn-on and turn-off losses and the diode reverse recovery losses are added to estimate the total switching loss:

$$P_{\text{sw, total}} = P_{\text{sw, IGBT(on)}} + P_{\text{sw, IGBT(off)}} + P_{\text{sw, diode}}. \quad (8)$$

The losses experienced by the power devices is modelled on only one module. As the inverter operation is symmetrical, this is scaled to all the modules by multiplying with the number of modules. In this case, the total power loss of the inverter P_{inv} is given by the equation:

$$P_{inv} = 6 \times (P_{cond} + P_{sw}) \quad (9)$$

The advantage of using this approach to calculate the approximate switching and conduction loss is that the coefficients required for calculation can be extracted directly from the datasheet of the power electronic module. However, the current varies at flux weakening region and it is important to calculate the current flowing to the motor under different operating conditions.

C. Current Calculation

Current calculation should be calculated in two separate ways for the low speed region and the high speed region with field weakening. At low speeds, $I_d = 0$ control is used to achieve Maximum Torque per Ampere (MTPA). At higher speed, the motor operates at constant power with field weakening.

1) Low Speed: In this case, all the current from the inverter is assumed to be applied on the q-axis. Hence i_q is taken to be the amplitude of the AC output current, which is related to the DC current drawn from the battery. The current amplitude can be calculated from the torque at the operation point via a proportion.

2) Field Weakening Region: In the field weakening region at high speed, it is assumed that constant power operation is realized while voltage is kept at the rated value. The current in the inverter is now estimated from the mechanical power by neglecting the losses:

$$I_{ph} = \frac{T\omega}{\sqrt{3}V_{rated}}. \quad (10)$$

D. Loss Coefficient Identification

Particle Swarm Optimisation (PSO) is a simple yet very powerful optimisation algorithm which utilises only primitive mathematical operators making it computationally faster with low memory requirement [8]. A PSO algorithm has a population (called swarm) of candidate solution (called particles). This computational method tries to improve the candidate solution by continuously moving the particles in a search space according to few mathematical formulae which helps determine its new position and velocity in the search space [9].

The PSO algorithm as shown in Figure 2 is used to identify the loss coefficients in the loss models. The vector $x_i(t)$ denotes the position of the i-th particle in the time step t. The elements of the vector are the loss coefficients: k_c, k_h, k_{ed}, and k_w in (4). Each of the particles has a velocity

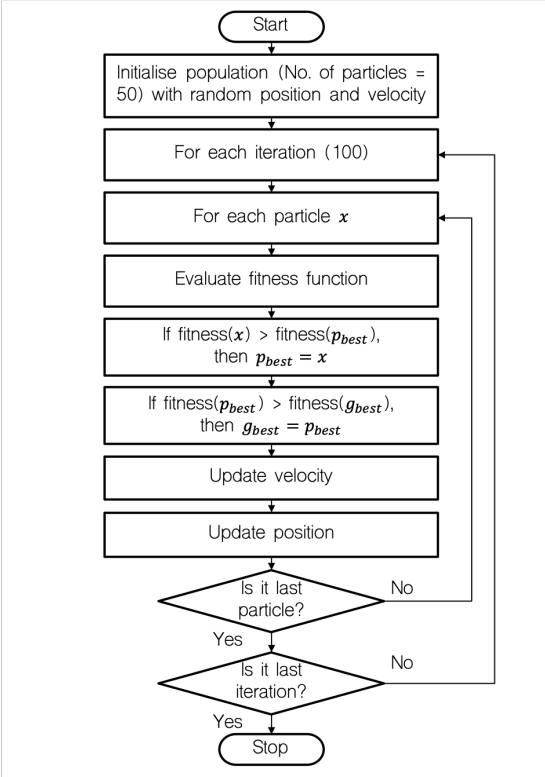

Fig. 2. Flowchart of PSO Algorithm [10].

associated to it along with its position denoted by $v_i(t)$. Velocity defines the movement of the particle in the search space which includes direction, distance and step size. In this technique, the particles interact with each other to find the best solution. The fitness function is defined to to maximize the match between the efficiency map plotted using the loss constants and the reference efficiency map. A total of 100 iterations with a swarm size of 50 particles are used to identify the coefficients. To observe the randomness of the initialisation and convergence of solution, the program can be repeatedly run for five times, showing the same converged results with different initial values, as can be seen from Figure 3.

The coefficients identified are $k_w = 0.001882$, $k_h = 14.7255$, $k_{ed} = 0.003641$, $k_w = 1.7761 \times 10^{-5}$. Figure 4 shows an error plot by taking the difference between the calculated efficiency map based on the identified coefficients and the reference efficiency map. It can be seen that In majority of the torque-speed region, the error is below 0.5%. The error in the low torque and low speed regions is relatively larger because of the non-linearities which are not considered and other assumptions made in the loss modelling.

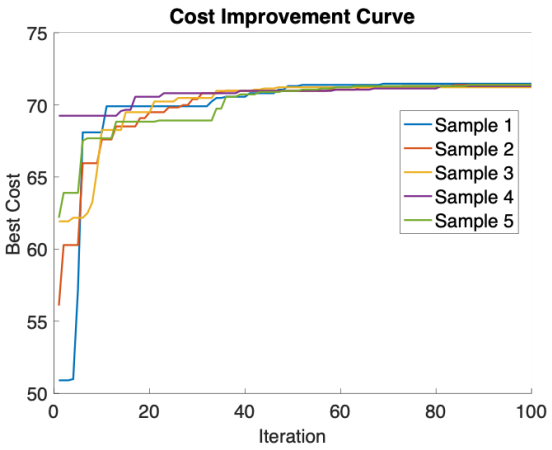

Fig. 3. Cost improvement curve for five sample runs of the PSO algorithm.

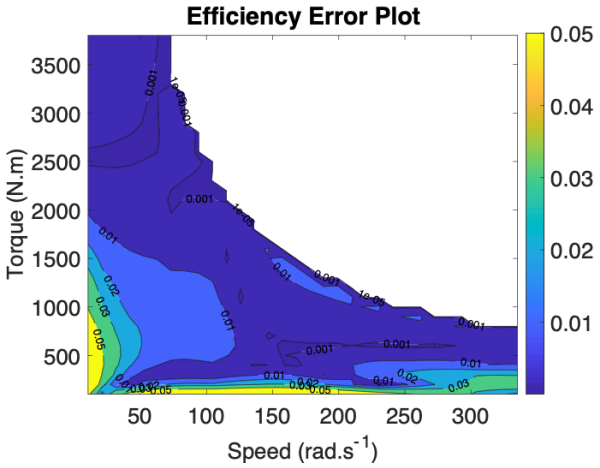

Fig. 4. Error between the calculated efficiency map and the reference efficiency map.

III. Sensitivity Study and Result Investigation

A forward-facing powertrain model is built using the obtained loss models. The model takes the drive cycle data as an input and includes the driver model, motor drive model, battery model, vehicle dynamic model and the transmission model. The vehicle parameters are retained from the information obtained from the manufacturers data. From the simulation, the energy efficiency of the heavy-duty BEV is obtained and is validated with the real world data from the manufacturer. The drive cycle used is from a real world test carried out by DAF for a heavy duty electric truck. The motor drive operating points in the studied drive cycle shown in the calculated efficiency map are presented in Figure 5. It can be seen a considerable portion of the operation points fall out of the peak efficiency region, which indicates there is space to improve the energy efficiency of the powertrain.

To perform the sensitivity analysis, a range of parameters are identified that have a significant influence on the energy efficiency of a heavy-duty BEV [11]. Table II shows the list of most sensitive parameters identified and the percentage

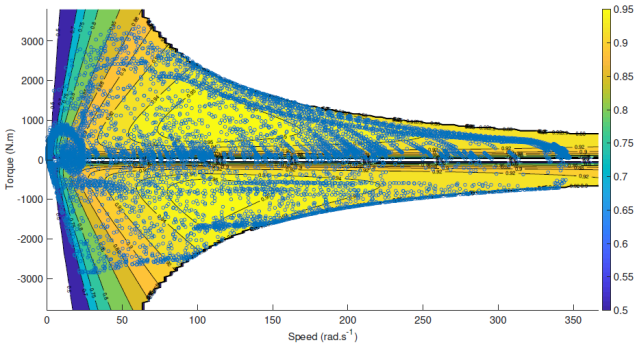

Fig. 5. Operation points of the motor drive shown in the efficiency map under the studied drive cycle.

increase in the BEV range for a 5% change of the vehicle parameter. For the radius of the wheel and transmission efficiency, 5% is increased from the reference value while for other parameters (mass, coefficient of rolling resistance, auxiliary power) 5% is decreased.

It can be seen that the truck mass and coefficient of rolling resistance are the most influencing parameters. Based on design choices, a wheel with a larger radius and the energy efficient auxiliary system will improve the range. Figure 6 shows the share of different losses calculated from the loss models with two wheel radii, which is impossible to be obtained from a conventional efficiency map approach. It can be seen that the major difference in losses is contributed by the motor, rather than the inverter. The loss components that are directly dependent on the speed of the motor such as hysteresis, eddy current, and windage loss are reduced when a bigger wheel is used. As expected, the copper losses increase for the bigger wheel as higher torque/current is drawn from the motor. It would be interesting to further optimize the powertrain for the studied drive cycle by optimizing the motor considering the radius of the wheel. Finally, opting for the most aerodynamic body for the truck and energy efficient design of auxiliaries are promising ways to improve the energy efficiency.

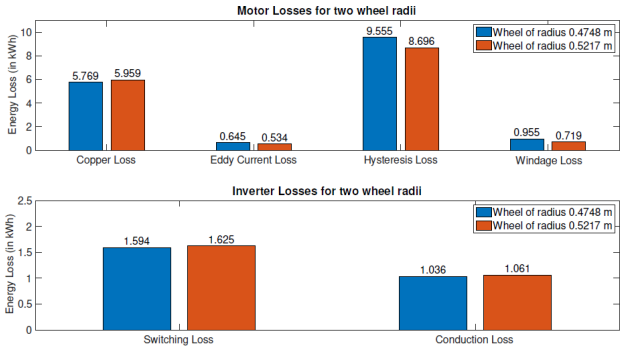

Fig. 6. Loss breakdown of two wheel radius configurations.

TABLE II
INCREASE IN RANGE FOR A 5% CHANGE IN VEHICLE PARAMETERS

Parameter	% Increase in Range
Truck mass	7.98
Rolling Resistance Coefficient	7.32
Radius of the wheel	6.13
Transmission Efficiency	3.64
Auxiliary System	1.73
Aerodynamic drag	1.30

IV. POWERTAIN ARCHITECTURE COMPARISON

In this research, two kinds of powertrain architectures are compared and modelled to analyse the improvement in the energy efficiency of the BEV. The two architectures are: two-speed transmission with a 200 kW single motor powertrain and dual-motor powertrain with two 160 kW motors. These two architectures are chosen over other options owing to its advantage of simplicity in design and implementation for a production vehicle.

A. Single motor powertrain with two-speed transmission

Two gears of different gear ratios are chosen by trial and error with the focus to improve the energy efficiency. In the simulation result presented, the gear shift from first gear to second is at speed of 35 km/h. For this study, the transmission efficiency is assumed to be the same as the efficiency of a fixed-gear transmission. The first gear is retained from the previous model and the second gear is taken to be of lower gear ratio. By doing so, the operation points are more concentrated to the peak efficiency region in the center of the efficiency map. From Table III, it can be seen that by using this two-speed transmission, the energy efficiency can be improved by 1.75%. Further study in this architecture can be seen in [12], [13], [14], [15].

B. Dual motor drive system

The powertrain architecture modelled is a dual-motor powertrain with all-wheel-drive capabilities which implies that a motor is attached in the front and rear axle via a fixed reduction gear [16], [17]. Two 160 kW motors from Siemens ELFA series are used from this architecture and IGBT modules compatible to these motors are chosen. The efficiency maps for 160 kW motors are not available and hence, the efficiency map of 200 kW motor is fitted into the torque-speed graph of the 160 kW motor by changing the y-axis scale from 0-3800 Nm of 200 kW motor to 0-2500 Nm to match the torque limits of 160 kW motor. This efficiency map was used as a reference efficiency map in the PSO algorithm to extract the motor loss constants. It is to be noted that this efficiency map is based on assumption and could be different from the actual values.

The dual motor powertrain model with two 160 kW motor is simulated with the updated motor and inverter specifications. From the simulation results in Table III, it can be seen that 9.11% improvement is seen in a dual-motor powertrain when compared to the 200 kW single motor powertrain. One of the main reason for this improvement in energy efficiency is that both the 160 kW motors operate at closer to the peak efficiency region in the center of the efficiency map. As can be seen from Figure.

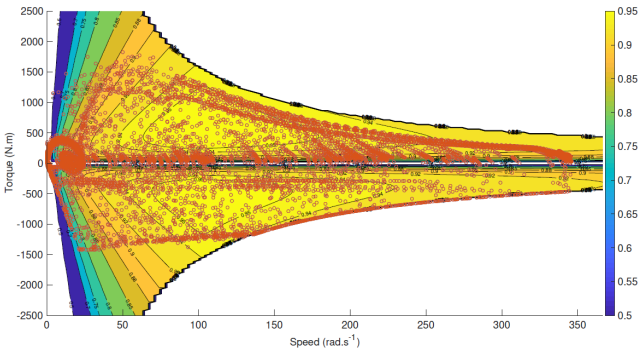

Fig. 7. Operation points of the 160 kW motor in the dual-motor powertrain.

TABLE III
ENERGY EFFICIENCY COMPARISON BETWEEN DIFFERENT POWERTRAIN ARCHITECTURES

	Energy Efficiency [kWh/km]	Range for 150 kWh battery pack [km]
200 kW Single-motor single-speed powertrain	1.4514	103.35
200 kW Single-motor two-speed powertrain	1.4265	105.15
160 kW Dual-motor powertrain	1.3301	112.77

V. CONCLUSION

This paper demonstrates the use of the PSO algorithm to extract the motor and inverter losses from an efficiency map of a PMSM drive. This algorithm has proven to be computationally inexpensive and fast in approaching optimal solution. Compared to directly using the efficiency map for powertrain simulation, the proposed loss model approach provides more insight into the sources and sharing of the losses without sacrificing the computational time.

The paper also presents the key parameters that have the most influence on the energy efficiency of a heavy- duty vehicle by carrying out a sensitivity study. Truck mass and rolling resistance coefficient are identified as the most sensitive parameters. Up to 7.98% and 7.32% increase in range was observed respectively for a 5% change from the base value of each of the parameters. From the other four parameters considered, opting to increase the wheel radius, improve the powertrain efficiency, utilise an efficient auxiliary system and reduce the aerodynamic drag coefficient improves the overall energy efficiency in the mentioned order. Among the different powertrain architectures, dual motor drive system with all-wheel-drive capabilities shows an improvement of 9.11% and single motor powertrain with two-speed transmission shows an improvement of 1.75% in the energy efficiency of the heavy-duty electric vehicle.

ACKNOWLEDGMENT

The authors would like to thank DAF Trucks NV for providing data and facilitating the research.

REFERENCES

[1] J. Landivar Lopez, "Hardware in the Loop Simulation of an Electric Vehicle Powertrain," Master's thesis, Delft University of Technology, Delft, The Netherlands, 2019.

[2] B. Bilgin, J. Liang, M. V. Terzic, J. Dong, R. Rodriguez, E. Trickett, and A. Emadi, "Modeling and Analysis of Electric Motors: State-of-the-Art Review," *IEEE Trans. Transport. Electrific.*, vol. 5, no. 3, pp. 602–617, Sep. 2019. [Online]. Available: https://ieeexplore.ieee.org/document/8772178/

[3] A. Boglietti, A. Cavagnino, M. Lazzari, and M. Pastorelli, "Predicting iron losses in soft magnetic materials with arbitrary voltage supply: an engineering approach," *IEEE Trans. Magn.*, vol. 39, no. 2, pp. 981–989, Mar. 2003.

[4] F. Fiorillo and A. Novikov, "An improved approach to power losses in magnetic laminations under nonsinusoidal induction waveform," *IEEE Trans. Magn.*, vol. 26, no. 5, pp. 2904–2910, Sep. 1990.

[5] L. Mestha and P. Evans, "Analysis of on-state losses in PWM inverters," *IEE Proceedings B - Electric Power Applications*, vol. 136, no. 4, pp. 189–195, Jul. 1989.

[6] E. A. Grunditz and T. Thiringer, "Modelling and scaling procedure of a vehicle electric drive system," *Report, Chalmers University of Technology, Sweden, url: https://research. chalmers. se/en/publication*, p. 19, 2017.

[7] A. Wintrich, U. Nicolai, W. Tursky, and T. Reimann, *Application manual power semiconductors*, 2nd ed. Ilmenau: ISLE Verlag, 2015.

[8] J. Kennedy and R. Eberhart, "Particle swarm optimization," in *Proceedings of ICNN'95 - International Conference on Neural Networks*, vol. 4, Nov. 1995, pp. 1942–1948 vol.4.

[9] R. Eberhart and J. Kennedy, "A new optimizer using particle swarm theory," in *MHS'95. Proceedings of the Sixth International Symposium on Micro Machine and Human Science*, Oct. 1995, pp. 39–43.

[10] B. Choudhury, S. Manickam, and R. M. Jha, "Particle Swarm Optimization for Multiband Metamaterial Fractal Antenna," *J. Optim.*, vol. 2013, p. 989135, Apr. 2013, publisher: Hindawi Publishing Corporation. [Online]. Available: https://doi.org/10.1155/2013/989135

[11] J. Asamer, A. Graser, B. Heilmann, and M. Ruthmair, "Sensitivity analysis for energy demand estimation of electric vehicles," *Transportation Research Part D: Transport and Environment*, vol. 46, pp. 182–199, Jul. 2016. [Online]. Available: https://linkinghub.elsevier.com/retrieve/pii/S1361920915300250

[12] A. Sorniotti, T. Holdstock, G. L. Pilone, F. Viotto, S. Bertolotto, M. Everitt, R. J. Barnes, B. Stubbs, and M. Westby, "Analysis and simulation of the gearshift methodology for a novel two-speed transmission system for electric powertrains with a central motor:," *Proceedings of the Institution of Mechanical Engineers, Part D: Journal of Automobile Engineering*, Jan. 2012. [Online]. Available: https://journals.sagepub.com/doi/10.1177/0954407011431415

[13] G. Wu, X. Zhang, and Z. Dong, "Impacts of Two-Speed Gearbox on Electric Vehicle's Fuel Economy and Performance," SAE International, Warrendale, PA, SAE Technical Paper 2013-01-0349, Apr. 2013. [Online]. Available: https://www.sae.org/publications/technical-papers/content/2013-01-0349/

[14] Q. Ren, D. Crolla, and A. Morris, "Effect of transmission design on Electric Vehicle (EV) performance," in *2009 IEEE Vehicle Power and Propulsion Conference*, Sep. 2009, pp. 1260–1265.

[15] B. Eberleh and T. Hartkopf, "A high speed induction machine with two-speed transmission as drive for electric vehicles," in *International Symposium on Power Electronics, Electrical Drives, Automation and Motion, 2006. SPEEDAM 2006.*, May 2006, pp. 249–254.

[16] G. Wu, X. Zhang, and Z. Dong, "Powertrain architectures of electrified vehicles: Review, classification and comparison," *J. Franklin Inst. B*, vol. 352, no. 2, pp. 425–448, Feb. 2015. [Online]. Available: http://www.sciencedirect.com/science/article/pii/S0016003214001288

[17] C. Rossi, D. Pontara, M. Bertoldi, and D. Casadei, "Two-motor, Two-axle Traction System for Full Electric Vehicle," *World Electric Vehicle Journal*, vol. 8, no. 1, pp. 25–39, Mar. 2016. [Online]. Available: https://www.mdpi.com/2032-6653/8/1/25